

# Potable Water Fluoride Rapid Detection Based on TBAF Desilylation by a Novel Fluorogenic 7-O-tert-butyldimethylsilyl-3-cyano-4-methylcoumarin Compound

Akumu Edwin Otieno\*<sup>1, 2</sup>, Barasa Stephen<sup>1</sup>, Lutta Samwel<sup>1</sup> and Akeng'a Teresa<sup>1</sup>

Department of Chemistry and Biochemistry, University of Eldoret,

P.O Box 1125-30100, Eldoret-Kenya

<sup>2</sup>Department of Physical and Biological Sciences, Kabarak University, Private bag-20157, Kabarak

\*Corresponding author's email address: oakumu@kabarak.ac.ke

#### Abstract

This article reports the synthesis and properties of a novel fluoride detector, 7-Otertbutyldimethylsilyl-3-cyano-4-methylcoumarin, which emits a lavender blue fluorescence in aqueous solution when fluoride ions are present. Bk-F93 F2000 Fluorospectrophotometer (FS), MRC-UV-Vis *Spectrophotometer-UV-(11S/N;* UEB1011006), GC micromass spectrometer (Micromass, Wythenshawe, Waters, Inc. UK), and Bruker Avance NEO 500 MHz (TXO cryogenic probe) NMR spectrometers were used for the spectral study. MestreNova (v14.0.0) program was used to process the NMR spectra. This sensor is highly specific and sensitive to water - soluble fluoride. The findings also show that fluoride doses as minimal as  $0.18 \mu M$  (3.42 x $10^{11}$  $mgL^{-1}$ ) can be reliably measured almost immediately, as shown by  $2^{nd}$  order rate constant of 1.9 x10 M<sup>-1</sup>min<sup>-1</sup>, in comparison to most fluoride sensors' range of 0.54 -116M-1min-1. The synthetic compound's responsiveness as a fluoride probe in the presence of other competing anions indicated no direct detection interference by any of evaluated ionic species. Thisfluoride probe demonstrated a higher quantum yield than the selected standard (quinine sulfphate), with values of  $\Phi = 0.65$  and  $\Phi = 0.54$ , 7-O-tertbutyldimethylsilyl-3-cyano-4respectively. Fluoride screening with methylcoumarin is simple and fast compared to conventional approaches that involve professional staff. As a result, the approach outlined herein is applicable and incredibly useful for assessing the quality of potable water in communities.

**Keywords:** Fluoride, sensor, potable water, 7-O-tert-butyldimethylsilyl-3-cyano-4-methylcoumarin

#### INTRODUCTION

Fluorescence spectroscopy as an analytical instrument has been extensively applied in many fields, including their use as fluorescence probes with elevated responsive activity based on their electronic properties, have seen an increase in scientific research attention in recent decades. (Panagopoulou *et al.*, 2020). There is a growing interest in highly selective and sensitive chromogenic as well as fluorogenic chemosensors for anions of biochemical significance (Kim et al., 2011; Said *et al.*, 2019). A typical chemosensor has a receptor that is connected to a fluorophore, which converts receptor detection into a fluorescence signal (*Guo et al.*, 2021; *Hu et al.*, 2021).

Due to their low cost and ease of identification of aqueous anions, chemical probes with an ability to produce visible response on a reaction with anion receptor are highly feasible (Dev *et al.*, 2018). An ideal fluorogenic fluoride detector must react selectively

and sensitively (Udhayakumari, 2019)to F in a device through effective fluorescence transduction mechanisms (Germani et al., 2020). These pathways include electron transfer upon analyte binding by the sensor, such as photoinduced electron transfer (PET) (Sun *et al.*, 2019), intramolecular charge transfer (ICT) (Lu *et al.*, 2019), fluorescence resonance energy transfer (FRET) (Meng *et al.*, 2019) and intramolecular proton transfer in the excited-state (ESIPT) (Fang *et al.*, 2019).

ICT imparts a huge impact in both the excitation and emission bands(Manna et al., 2018). It represents the degree of contact between the Donor and the Acceptor (Fig. 1). In terms of fluorescence reaction recognition mechanisms, PET probes vary from ICT probes. Unlike ICT, quenching in PET does not result in fluorescence band changes. In contrast, FRET involves the transfer of excitation frequency (Fig. 2). ESIPT is most commonly observed in structures with a five- or six-membered rings that undergo tautomerization with a broad Stokes shift. As chromophores resist the inner filter effect, fluorescence analysis in ESIPT improves (Fig. 3) (Jiao et al., 2015).



Figure: 1. ICT mechanism in designing fluorogenic probes

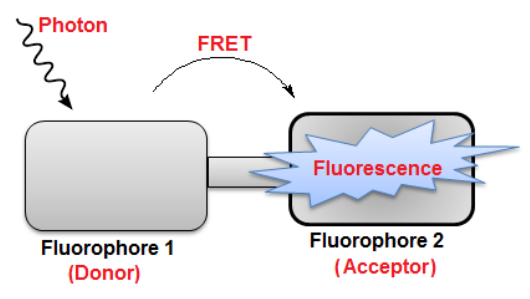


Figure: 2. FRET mechanism in designing fluorogenic probes

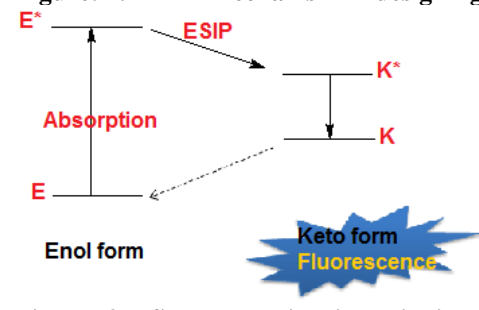


Figure: 3. ESIP mechanism in designing fluorogenic probes

Coumarins are one kind of fragrant organic fluorogenic probe dependent on ICT mechanism. Due of their outstanding compatibility with biological systems, solid and steady fluorescence, and excellent functional stability, these compounds are often used in the development of small-molecule fluorescent chemical sensors. (Cao *et al.*, 2018). When excited, the ICT process takes place, and fluorescence occurs(Liese & Haberhauer, 2018). Ses compounds become non-fluorescent as they are protected by trialkylsilyloxy group. In the presence of fluoride ion, the protecting moiety is lost leading to the dye being switched back on (Jiao *et al.*, 2015). Another promising

approach for creating versatile fluoride fluorescence sensors is focused on the forming of potent attachment of fluoride to the trialkylsilyloxy residues via Si-O bond cleavage. (Chansaenpak et al., 2018). Centered on tetra-n-butylammonium fluoride (TBAF) promoted desilylations, we report the synthesis and fluorescence characteristics of a novel versatile and highly discriming fluorogenic fluoride ion probe.

#### METHODOLOGY

## Synthesis of 7-O-tert-butyldimethylsilyl-3-cyano-4-methylcoumarin

3-cyano-4-methylcoumarin (30g, 0.15mol) also referred to here as compound 1 and imidazole (20.4g, 0.3mol) were dissolved in a 600 mL mixture (3:1) of dry dichloromethane (DCM)-Tetrahydrofuran (THF) solvent. This solution was then continuously stirred in an inert atmosphere of  $N_2$  gas until the solution became clear. Tert-butyldimethylsilylchloride (TBDMS, 22.6g, 0.15mol) in 60 mL of dichloromethane was slowly added dropwise for three continuous hours. This process was allowed to take place for an extra 2 hours at room temperature with agitation and in an inert environment.

This followed by filtration through a short celite bed and washed three times with 600 mL of purified and deionized water, supplemented by 200 mL of aqueous NaCl. The non-polar fraction was then dried by exposure to anhydrous sodium sulphate, filtered and concentrated using a Buchi rotavapour under reduced temperature and pressure to get an unpurified product. Further purification was done by means of column chromatography using DCM:THF as a mobile phase in varying concentrations. The result obtained at this stage was a bright yellow crystalline solid. These crystals were again subjected to further purification through another column using DCM:THF solvent system. This second column purification was done more cautiously, and only the central portions of the fractions were selected and concentrated. Upon concentration and drying under decreased pressure and high vacuum for an extended period of time, the product was collected as a bright and shiny yellow solid, 24.67 g (82.24% yield). A scheme on the synthesis of compound 2 is presented in Fig. 4 below.

Figure 4: Schematic of 7-O-tert-butyldimethylsilyl-3-cyano-4-methylcoumarin (2) synthesis

## Fluorescence Fluoride testing

Colorimetric and fluorescent examination is used to investigate the interaction between compound **2** and fluoride ions (fig. 5) in dioxane solution. A number of fluoride concentrations (0.1 - 100 mg/L) were made from TBAF. To each of these solutions, 1 mL of a 4 percent compound **2** solution prepared in dioxane was added. These solutions were incubated for 15 minutes at room temperature in 1:1 (v/v) 10 millimolar solutions of HEPES in dioxane maintaining the pH at 7.4. These solutions produced fluorescence spectra with excitation wavelength of  $3.32 \times 10^{-7}$ m and emission wavelength of and  $3.6 \times 10^{-7}$ m.

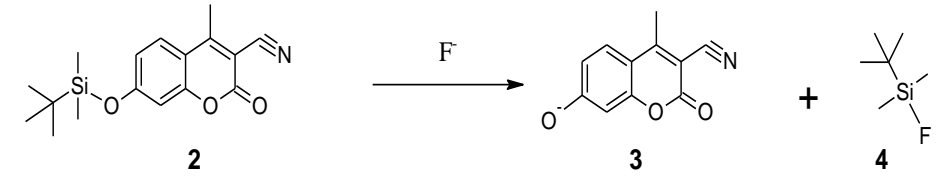


Figure 5: Schematic of desilylation of 7-O-tert-butyldimethylsilyl-3-cyano-4-methylcoumarin

# **Selectivity studies**

Varying concentrations of a number of selected anions; chloride, bromide, iodide, nitrate ans sulphate at a concentration of 200  $\mu M$  were prepared as well as TBAF and NaF (200  $\mu M$ ). The studies were done in a solution of a pH maintained at 7.4 by 1:1 (v/v) 10 mM HEPES: dioxane mixture. A number of [F] of this probe (0.1 to 100 mg/L) were prepared from TBAF. 1 mL of a 4 % solution of each of the synthesize compound contained in dioxane was mixed with 40 mL of test samples containing the fluorideions. This was followed by a 20 minutes incubation at room temperature. Fluorescence studies in terms of excitation and emission frequencies were done for each of these solutions. Three replicates were tested for each anion.

## **Quantum Yield**

The intensity of fluorescence of compound  $2 + F^-$  was measured at the excitation wavelength of  $4.55 \times 10^{-7}$ m while maintaining the absorbance at  $\le 0.05$  in order to avoid self-quenching. Quantum yield was determined using eq 1.

$$\Phi_X = \Phi_{ST} \left( \frac{\operatorname{Grad}_X}{\operatorname{Grad}_{ST}} \right) \left( \frac{\eta_X^2}{\eta_{ST}^2} \right) \dots 1$$

Where:

 $\Phi$  = quantum yield,

 $\eta =$ solvent refractive index,

ST = standard (quinine sulfate dihydrate in this case)

X = unknown.

A plot of absorbance versus the area was done and used for quantumyield calculations. The fluorescence reference used for this study was quinine sulfate dihydrate (AnaSpec) in  $1x10^{-1}$  Molar perchloric acid (Nawara & Waluk, 2019) with a quantum yield of 54.6% (excitation. =  $3.1x10^{-7}$ m, emission. =  $4.55x10^{-7}$ m) (Wang et al., 2019).

## Paper Disc Assays.

Paper discs were made by punching Whatman filter paper ( $20~\mu m$ ) into small discs. The paper discs were soaked into a 1:3 THF: DCM solvent mixture containing two millimolar concentration of compound (2) and dried. The dry pretreated filter paper discs were soaked in 2 millimolar cetyltrimethylammonium bromide, CTAB for five seconds and allowed to dry. A portable UV lamp was used to observe the fluorescence on the paper discs below 365 nm (UVGL-58 from UVP). For specificity tests on compound (2), an artificial aquifer was made with double the required amount of NaF in the analysis. The analyte was combined with 2 millimolar CTAB in 10 millimolar acetate in the ratio of 1:1 (v/v).

#### RESULTS AND DISCUSSION

#### Spectral information on compound 2

<sup>1</sup>HNMR (500 MHz, MeOD): δ 1.38 (6H, s), 2.16 (9H, s), 2.73 (3H, s), 6.92 (1H, dd, J = 7.7, 1.5 Hz), 6.76 (1H, d, J = 1.5, 0.5 Hz), 7.79 (1H, d, J = 7.7, 0.5 Hz).

<sup>13</sup>CNMR: (500 MHz, MeOD): δ 1.66, 15.36, 15.76, 28.51, 101.28, 110.01, 112.88, 113.22, 127.18, 154.70, 157.33, 162.57 and 163.78.

The <sup>1</sup>HNMR (500 MHz, MeOD) spectrum showed different multiplicities. The aliphatic protons resonate at  $\delta$  1.38 (6H, s), 2.16 (9H, s) and 2.73 (3H, m), while the aromatic protons at 6.92 (1H, dd, J = 7.7, 1.5 Hz), 6.76 (1H, d, J = 1.5, 0.5 Hz), 7.79 (1H, d, J = 7.7, 0.5 Hz). The <sup>1</sup>H–<sup>1</sup>H coupling was observed between  $\delta$  7.79 and  $\delta$  6.92 while two-bond coupling ( $^{1}$ H–C– $^{1}$ H) were between  $\delta$  6.76 and  $\delta$  6.92. The multiplicity indicated that the aromatic proton at is coupled to the two other protons at  $\delta$  7.79 and  $\delta$  6.76, thus the signal at  $\delta$  6.92 is a double duplet. The aromatic proton at  $\delta$  7.79 only shows coupling with another at 6.76 hence is a duplet. The non-aromatic protons at  $\delta$  1.38,  $\delta$  2.16 and  $\delta$  2.73 all show no coupling and appear as singlets. The Mass spectrum revealed an M<sup>+</sup> + 1 at 316.9. A single diode array peak at 2.92 retention time on this compound confirms its purity.

## Fluorescence properties

The analyte's fluorescence intensity was quantified by studying the absorption wavelength at  $3.32 \times 10^{-7} \text{m}$  as well as emission wavelength at and  $3.6 \times 10^{-7} \text{m}$ . Compound (2) therefore, registered a stokes shift of 28nm (Fig. 6). The change in fluorescence intensity with increasing fluoride ion concentration. This plot is dependent on fluoride test measurements from a replicate of three. The result revealed that the fluorescence strength has a linear correlation with fluoride concentration, suggesting a 1:1 stoichiometric ratio between fluoride ions and compound (2). The fluorescence intensity at 200 sec for compounds calculated by substituting time in seconds into the linear equation (y = -0.0202x + 5.1725) in figure 7 yielded a 1.13 AFU.

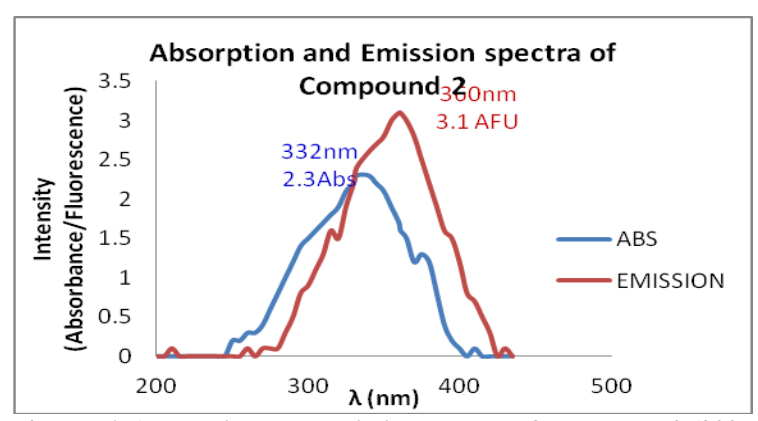


Figure: 6. Absorption and Emission spectra of compound 2 (200  $\mu M$ ) in F  $^{\text{-}}$  free solution.

#### **Detection Limit and Selectivity**

An investigation on the Fluoride limit of detection by compound (2) in TBAF confirmed its capacity to resolve TBAF dosages as low as  $0.18~\mu M~(3.42~x10^{11}~mgL^{-1})$ . The response of compound (2) to declining aqueous concentrations NaF in a water: dioxane solvent mixture in the ratio of 1:1 (v/v) led to an observation on detection limit of  $4.5~\mu M~(8.55x10^{11}~mgL^{-1})$ . This is much lower than the recommended WHO levels for fluoride concentration in drinking water  $789.4~\mu M~(1.5mgL^{-1})$ . The response of compound 2 as a fluoride sensor in the presence of other anions (Cl<sup>-</sup>, Br<sup>-</sup>, I<sup>-</sup>, NO<sub>3</sub><sup>-</sup>, and  $SO_4^{-2}$ ) did not reveal any direct competition with any of the tested anions (Fig. 7). The

results undoubtedly show that environmentally relevant anions present in groundwater have negligible interference to fluoride sensing by compounds 2.

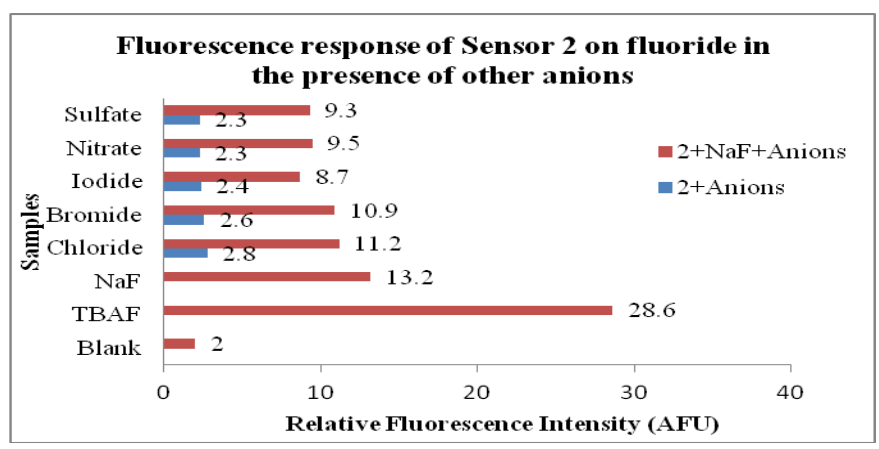


Figure 7: Selectivity of compound 2 (20  $\mu M)$  for fluoride in the existence of other anions

The 2<sup>nd</sup> order rate constant was established to be 1.9 x10 M<sup>-1</sup>min<sup>-1</sup> demonstrating the ability of compound **2** to rapidly detect the presence of aqueous fluorides in portable water as compared to a range of 0.54 M<sup>-1</sup>min<sup>-1</sup> to 116 M<sup>-1</sup>min<sup>-1</sup> for most fluoride sensors (Zheng et al., 2016).

#### **Quantum vield**

The quantum yield of compound 2 was higher than the standard (quinine sulfphate) at 0.65 and 0.54 respectively. This value was calculated by measuring the integrated Fluorescence intensity of sample in dioxane (refractive index  $\eta$ = 1.42) against quinine sulphate in 0.1M perchloric acid (refractive index  $\eta$ = 1.33) as standard (fig.8) this indicates that compound 2 has a higher efficiency of photon emission than Quinine sulphate.

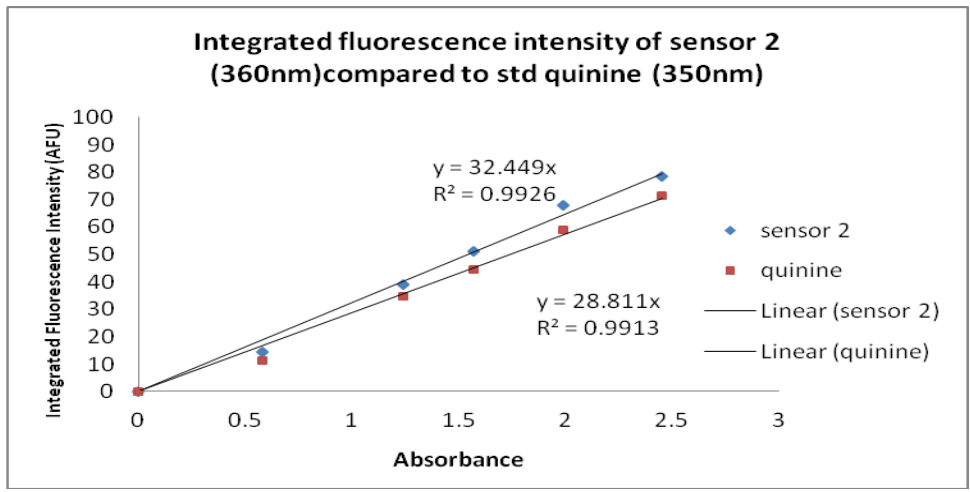


Figure 8: Plot of integrated Fluorescence intensity of sensor 2 versus the corresponding absorbance for the standard (quinine sulphate)

Paper Disc-Based Sensing of Fluoride in Aqueous Samples

Since we target portable water, we envisioned the use of test paper discs as cheap and therefore can be easily accessible fluoride probes. This can be done by monitoring the fluorescence changes in the probe. The addition of TBAF to compound (2) contained in dioxane generated observable changes in both excitation spectrum as well as the emission spectrum, resulting in a deprotected product (Fig. 9).

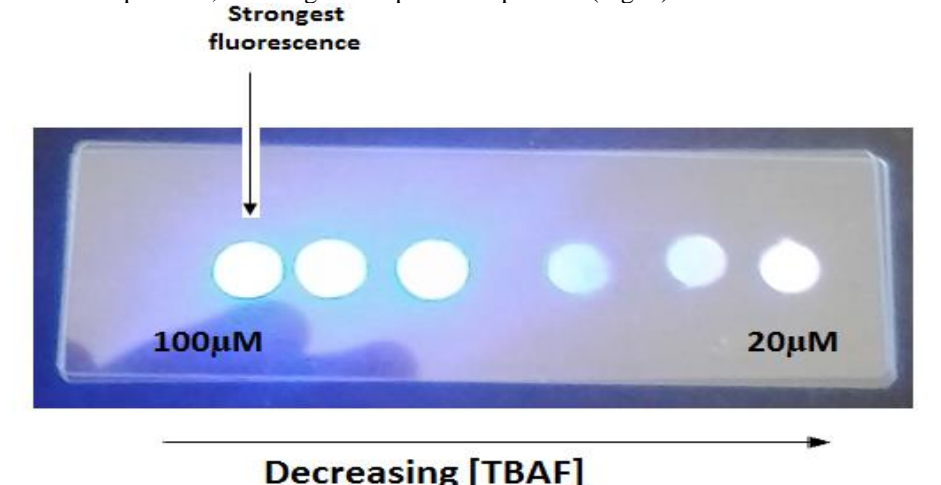


Figure 9. Fluorescence variations of paper discs containing the compound (2) in TBAF This paper disc-based test was also able to resolve fluoride when other anions notably (Cl<sup>-</sup>, Br<sup>-</sup>, I<sup>-</sup>, NO<sub>3</sub><sup>-</sup>, and SO<sub>4</sub><sup>-2</sup>) were present. These findings suggest that the 7-O-tert-butyldimethylsilyl-3-cyano-4-methylcoumarin scaffold has the potential to be a robust architectural blueprint for designing new customized fluoride sensors. Finally, the paper disc-based test mentioned above may be combined with portable fluorescence viewers to allow for speedy fluoride detection.

#### **CONCLUSION**

In conclusion, the synthesis of 7-O-tert-butyldimethylsilyl-3-cyano-4-methylcoumarin was successful. Its adaptability as a scaffold for the development of highly responsive and selective systems for fluoride measurement has been verified. This dye has great potential to sense fluoride in aqueous samples, allowing for simple fluoride analysis in the formal and informal environments at safe F<sup>-</sup> concentrations as recommended by WHO.

Owing to the poor solubility of 7-O-tert-butyldimethylsilyl-3-cyano-4-methylcoumarin in water, a paper disc-based analysis for fluoride was developed. This technique can theoretically be used for cheap fluoride analysis. The research findings here offer a simple but cheap, selective and sensitive tool for analyzing fluoride in water samples.

#### ACKNOWLEDGMENTS

Much thanks to the National Research Funds (NRF-Kenya Government.) for the financial support through this work. We also thank Kabarak University for the assistance in Fluorometry as well as Uppsala University for the MS and NMR Spectrometry. We also acknowledge helpful discussions with Chemistry Department, University of Eldoret.

#### REFERENCES

- Cao, X., Zhao, N., Lv, H., Gao, A., Shi, A., & Wu, Y. (2018). 4-Nitrobenzene thiourea self-assembly system and its transformation upon addition of Hg2+ ion: Applications as sensor to fluoride ion. *Sensors and Actuators B: Chemical*, 266, 637–644. https://doi.org/10.1016/j.snb.2018.03.188
- Chansaenpak, K., Kamkaew, A., Weeranantanapan, O., Suttisintong, K., & Tumcharern, G. (2018). Coumarin Probe for Selective Detection of Fluoride Ions in Aqueous Solution and Its Bioimaging in Live Cells. Sensors, 18(7), 2042. https://doi.org/10.3390/s18072042
- Dey, S. K., Al Kobaisi, M., & Bhosale, S. V. (2018). Functionalized Quinoxaline for Chromogenic and Fluorogenic Anion Sensing. *ChemistryOpen*, 7(12), 934–952. https://doi.org/10.1002/open.201800163
- Fang, H., Wang, N., Xie, L., Huang, P., Deng, K.-Y., & Wu, F.-Y. (2019). An excited-state intramolecular proton transfer (ESIPT)-based aggregation-induced emission active probe and its Cu(II) complex for fluorescence detection of cysteine. Sensors and Actuators B: Chemical, 294, 69–77. https://doi.org/10.1016/j.snb.2019.05.022
- Germani, R., Anastasio, P., Chiodini, M., Del Giacco, T., Tiecco, M., & Belpassi, L. (2020). Fluorescent signal transduction in a self-assembled Hg2+ chemosensor tuned by various interactions in micellar aqueous environment. *Journal of Photochemistry and Photobiology A: Chemistry*, 389, 112276. https://doi.org/10.1016/j.jphotochem.2019.112276
- Guo, C., Sedgwick, A. C., Hirao, T., & Sessler, J. L. (2021). Supramolecular fluorescent sensors: An historical overview and update. *Coordination Chemistry Reviews*, 427, 213560. https://doi.org/10.1016/j.ccr.2020.213560
- Hu, Y., Long, S., Fu, H., She, Y., Xu, Z., & Yoon, J. (2021). Revisiting imidazolium receptors for the recognition of anions: Highlighted research during 2010–2019. *Chemical Society Reviews*, 50(1), 589–618. https://doi.org/10.1039/DOCS00642D
- Jiao, Y., Zhu, B., Chen, J., & Duan, X. (2015). Fluorescent Sensing of Fluoride in Cellular System. Theranostics, 5(2), 173–187. https://doi.org/10.7150/thno.9860
- Kim, H. N., Guo, Z., Zhu, W., Yoon, J., & Tian, H. (2011). Recent progress on polymer-based fluorescent and colorimetric chemosensors. *Chem. Soc. Rev.*, 40(1), 79–93. https://doi.org/10.1039/C0CS00058B
- Liese, D., & Haberhauer, G. (2018). Rotations in Excited ICT States—Fluorescence and its Microenvironmental Sensitivity. *Israel Journal of Chemistry*, 58(8), 813–826. https://doi.org/10.1002/ijch.201800032
- Lu, G., Guo, Y., Zhuo, J., Li, X., Chi, H., & Zhang, Z. (2019). A General Strategy for Through-Bond Energy Transfer Fluorescence Probes Combining Intramolecular Charge Transfer: A Silyl Ether System for Endogenous Peroxynitrite Sensing. Chemistry – A European Journal, chem.201903880. https://doi.org/10.1002/chem.201903880
- Manna, A. K., Mondal, J., Rout, K., & Patra, G. K. (2018). A new ICT based Schiff-base chemosensor for colorimetric selective detection of copper and its copper complex for both colorimetric and fluorometric detection of Cysteine. *Journal of Photochemistry and Photobiology A: Chemistry*, 367, 74–82. https://doi.org/10.1016/j.jphotochem.2018.08.018
- Meng, H., Huang, X.-Q., Lin, Y., Yang, D.-Y., Lv, Y.-J., Cao, X.-Q., Zhang, G.-X., Dong, J., & Shen, S.-L. (2019). A new ratiometric fluorescent probe for sensing lysosomal HOCl based on fluorescence resonance energy transfer strategy. Spectrochimica Acta Part A: Molecular and Biomolecular Spectroscopy, 223, 117355. https://doi.org/10.1016/j.saa.2019.117355
- Nawara, K., & Waluk, J. (2019). Goodbye to Quinine in Sulfuric Acid Solutions as a Fluorescence Quantum Yield Standard. Analytical Chemistry, 91(8), 5389–5394. https://doi.org/10.1021/acs.analchem.9b00583
- Panagopoulou, M. S., Wark, A. W., Birch, D. J. S., & Gregory, C. D. (2020). Phenotypic analysis of extracellular vesicles: A review on the applications of fluorescence. *Journal of Extracellular Vesicles*, 9(1), 1710020. https://doi.org/10.1080/20013078.2019.1710020
- Said, A. I., Georgiev, N. I., & Bojinov, V. B. (2019). The simplest molecular chemosensor for detecting higher pHs, Cu2+ and S2- in aqueous environment and executing various logic gates. *Journal of Photochemistry and Photobiology A: Chemistry*, 371, 395–406. https://doi.org/10.1016/j.jphotochem.2018.11.029
- Sun, W., Li, M., Fan, J., & Peng, X. (2019). Activity-Based Sensing and Theranostic Probes Based on Photoinduced Electron Transfer. Accounts of Chemical Research, 52(10), 2818–2831. https://doi.org/10.1021/acs.accounts.9b00340
- Udhayakumari, D. (2019). Detection of toxic fluoride ion via chromogenic and fluorogenic sensing. A comprehensive review of the year 2015–2019. *Spectrochimica Acta Part A: Molecular and Biomolecular Spectroscopy*, 117817. https://doi.org/10.1016/j.saa.2019.117817
- Wang, Y., Mu, Y., Hu, J., Zhuang, Q., & Ni, Y. (2019). Rapid, one-pot, protein-mediated green synthesis of water-soluble fluorescent nickel nanoclusters for sensitive and selective detection of tartrazine. Spectrochimica Acta Part A: Molecular and Biomolecular Spectroscopy, 214, 445–450. https://doi.org/10.1016/j.saa.2019.02.055